Climate Dynamics (2003) 21: 689–698
DOI 10.1007/s00382-003-0355-z

J. C. Larrasoaña · A. P. Roberts · E. J. Rohling
M. Winklhofer · R. Wehausen

Three million years of monsoon variability over the northern Sahara

Received: 6 January 2003 / Accepted: 18 August 2003 / Published online: 21 October 2003

Abstract We present a 3 million year record of aeolian dust supply into the eastern Mediterranean Sea, based on hematite contents derived from magnetic properties of sediments from Ocean Drilling Program Site 967. Our record has an average temporal resolution of ~400 years. Geochemical data validate this record of hematite content as a proxy for the supply of aeolian dust from the Sahara. We deduce that the aeolian hematite in eastern Mediterranean sediments derives from the eastern Algerian, Libyan, and western Egyptian lowlands located north of the central Saharan watershed (~21°N). In corroboration of earlier work, we relate dust flux minima to penetration of the African summer monsoon front to the north of the central Saharan watershed. This would have enhanced soil humidity and vegetation cover in the source regions, in agreement with results from "green Sahara" climate models. Our results indicate that this northward monsoon penetration recurred during insolation maxima throughout the last 3 million years. As would be expected, this orbital precession-scale mechanism is modulated on both short (~100-kyr) and long (~400-kyr) eccentricity time scales. We also observe a strong expression of the ~41-kyr (obliquity) cycle, which we discuss in terms of high- and low-latitude mechanisms that involve Southern Hemisphere meridional temperature contrasts and shifts in the latitudes of the tropics, respectively. We also observe a marked increase in sub-Milankovitch variability around the mid-Pleistocene transition (~0.95 Ma), which suggests a link between millennial-scale climate variability, including monsoon dynamics, and the size of northern hemisphere ice sheets.

J. C. Larrasoaña · A. P. Roberts (✉) · E. J. Rohling
M. Winklhofer
School of Ocean and Earth Science,
Southampton Oceanography Centre,
University of Southampton, European Way,
Southampton SO14 3ZH, UK
E-mail: arob@mail.soc.soton.ac.uk

R. Wehausen
Institut für Chemie und Biologie des Meeres (ICBM),
Carl-von-Ossietzky-Universität,
26111, Oldenburg, Germany

1 Introduction

Orbital precession exerts a fundamental control on variations of aeolian (Saharan) dust supply into the eastern Mediterranean Sea, in such a way that organic-rich sediments (sapropels) deposited during precession minima, and marls deposited during maxima, coincide with periods of low and high dust supply, respectively (Emeis et al. 2000; Wehausen and Brumsack 2000; Foucault and Mélières 2000; Lourens et al. 2001; Dinarès-Turell et al. 2003). These cycles have been linked to changes in humidity over northern Africa associated with precession-related oscillations in the intensity of the African monsoon (Rossignol-Strick et al. 1982; Rossignol-Strick 1983, 1985). In this work, we address the specific climatic mechanism linking dust production and African monsoon variability, which has remained elusive.

A recent reconstruction of north African environmental conditions during the previous (Eemian) interglacial maximum (Rohling et al. 2002) offers a testable working hypothesis regarding this mechanism. Traditionally, the light $\delta^{18}O$ values observed within the majority of Quaternary sapropels have been attributed to increased Nile runoff during precession minima (Rossignol-Strick et al. 1982; Rossignol-Strick 1983). However, new $\delta^{18}O$ data from sapropel S5 (~124-119 ka BP) (Rohling et al. 2002) and results from many other late Quaternary sapropels (Fontugne et al. 1994; Emeis et al. 2003) demonstrate that the lightest $\delta^{18}O$ values are typically found between Libya and southwest Crete, rather than in the Nile River plume. To account for this observation, Rohling et al. (2002) proposed that significant northward penetration of the African summer monsoon beyond the central Saharan watershed

($\backsim$21°N) occurred simultaneously with enhanced monsoon flooding through the Nile, allowing direct and rapid drainage of low-δ^{18}O precipitation (Gasse 2000) from the African summer monsoon front along the wider north African margin into the eastern Mediterranean (particularly via the eastern Gulf of Sirte). Northward penetration of the African summer monsoon front beyond the central Saharan watershed ($\backsim$21°N) also forms a useful concept for explaining the observed modulation of aeolian dust supply into the eastern Mediterranean on precession time scales. Expansion of (savanna-like) vegetation cover ("greening of the Sahara", Claussen et al. 1998; Brovkin et al. 1998) would lead to an increase in the cohesiveness of soil particles throughout vast tracts of the northern Sahara, which would contribute to decreased dust production (Middleton 1985).

This hypothesis, which we seek to test here, would imply that one might gauge long-term variations in the intensity/penetration of the African summer monsoon by examining aeolian dust records from the eastern Mediterranean Sea. Available dust records (Emeis et al. 2000; Wehausen and Brumsack 2000; Foucault and Mélières 2000; Lourens et al. 2001; Dinarès-Turell et al. 2003), however, are short and non-overlapping, and consequently only provide time series for dust supply that are both spatially and temporally discontinuous. Moreover, they are based on different proxies (e.g. clay mineralogy, geochemistry, magnetic properties) whose cross-calibration in terms of dust source area is uncertain. Identification of the dust source area is essential if we are to establish the link between dust production and intensity/penetration of the summer monsoon.

We present a high-resolution proxy record of northern Saharan dust supply into the eastern Mediterranean Sea for the last 3 million years, which is based on magnetic measurements of continuously sampled cores from Ocean Drilling Program (ODP) Site 967 (ODP Shipboard Scientific Party 1996; Emeis et al. 2000). Site 967 was sampled because, of all the eastern Mediterranean ODP sites, it has been shown to be the most suitable for obtaining a long, high-resolution record of dust fluctuations (Wehausen and Brumsack 2000; Lourens et al. 2001). We interpret this record on the basis of a comprehensive multi-proxy magnetic, geochemical and δ^{18}O dataset. The observed oscillations of hematite content, by virtue of their high resolution and long temporal coverage (3 Myr), allow us to test the concept of northward penetration of the African summer monsoon beyond $\backsim$21°N at the full range of orbital variations.

2 Materials and methods

Site 967 was cored at a water depth of 2553 m on the northern slope of Eratosthenes Seamount (34°04′N, 32°43′E) (Fig. 1). The sediments between 0 and 89.5 revised metres composite depth (rmcd) consist of early Pliocene to Holocene hemipelagic bioturbated nannofossil oozes and nannofossil clays, and include 79 sapropels, a slumped interval between $\backsim$58 and 64 rmcd, and several thin (cm-dm) turbiditic layers that do not disrupt the sapropel stratigraphy (ODP Shipboard Scientific Party 1996; Kroon et al. 1998). We collected 72 continuous u-channel samples from the upper 89.5 m of the Site 967 record. All the measured intervals have been converted to the rmcd scale (Sakamoto et al. 1998). Use of the composite depth scale of Sakamoto et al. (1998), which is based on detailed correlation of physical properties among the holes cored at Site 967, is important because it provides a temporally continuous record on which spectral analysis can be performed. This enables us to examine the driving mechanisms of the measured dust signal.

The age model used for Site 967 is that of Kroon et al. (1998). This age model was developed by tuning the characteristic sapropel pattern to an orbital precession target curve and is constrained by

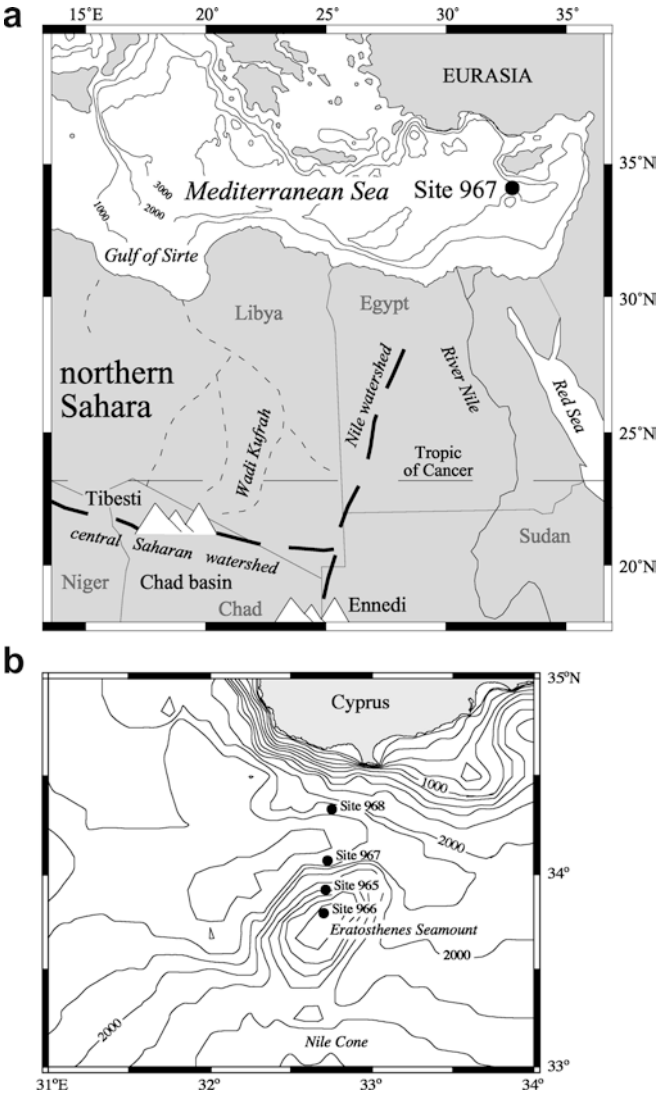

Fig. 1 **a** Map of the eastern Mediterranean Sea and northeastern Africa with location of the site studied and of the main northern Saharan geographic elements discussed in the text. **b** More detailed map of the location of Site 967 on the northern slope of Eratosthenes Seamount. Site 967 lies on a ridge that is elevated above the slope (see seismic reflection lines in Shipboard Scientific Party 1996), where deposition is consistent with hemi-pelagic settling from suspension

nannofossil datums (Staerker 1998) and by oxygen isotope data for the last million years, where the sapropel pattern is not as distinctive as before 1 Ma.

Magnetic measurements were made at 1-cm intervals with a narrow-access pass-through cryogenic magnetometer (Weeks et al. 1993) at the Southampton Oceanography Centre (SOC). The magnetic properties measured include an anhysteretic remanent magnetization (ARM; imparted with a dc bias field of 0.05 mT and a peak alternating field (AF) of 100 mT), an isothermal remanent magnetization ($IRM_{0.9\ T}$; imparted with an induction of 0.9 T) and a back-field $IRM_{-0.3\ T}$ (imparted with a back-field of 0.3 T). Variations in high coercivity mineral content are expressed by the "hard IRM" parameter (HIRM = $(IRM_{0.9\ T} - IRM_{-0.3\ T})/2$) (King and Channell 1991). Although consistent HIRM values were obtained for some intervals, unreliable $IRM_{0.9\ T}$ and $IRM_{-0.3\ T}$ values were obtained for many u-channels because the IRM intensities exceeded the dynamic range of the magnetometer. To avoid this problem and other uncertainties related to HIRM calculations (e.g. Liu et al. 2002), we developed a new proxy ($IRM_{0.9\ T}@AF_{120\ mT}$) for the concentration of hematite by AF demagnetizing the $IRM_{0.9\ T}$ at 120 mT. Thermal demagnetization of an IRM (imparted at 0.9 T) that had been AF-demagnetized at 120 mT was carried out for selected discrete samples to identify the high coercivity mineral(s) responsible for the $IRM_{0.9\ T}@AF_{120\ mT}$ signal.

Several spectral analysis techniques were employed to evaluate the temporal evolution of the dust signal. The results are presented in the form of a Lomb-Scargle power spectrum, along with a wavelet analysis (Torrence and Compo 1998) for the whole record. The wavelet power spectrum was computed to allow for the possibility that signals may not be purely periodical over the full time scale considered. The Lomb-Scargle power spectrum, which does not necessitate interpolation of data onto a regular grid, was used to select significant periods for band-pass filtering. Significance was established using red-noise estimates from a first-order autoregressive process. Band-pass filtered periods were compared with astronomical solutions for the orbital obliquity and precession parameter (Laskar et al. 1993). These values were normalized by their respective standard deviation; the solution for eccentricity was band-pass filtered to obtain separate solutions for long (400-kyr) and short (100-kyr) eccentricity, which were then also normalized by their standard deviation. The Matlab function "filtfilt" was used for zero-phase filtering of the $IRM_{0.9\ T}@AF_{120\ mT}$ record and the eccentricity solution, with a finite-impulse-response band-pass filter (using a 60 dB stop band).

3 Results

Thermal demagnetization data indicate that the high coercivity mineral in eastern Mediterranean sediments at Site 967 is hematite. For all samples, the magnetization completely unblocks at around 680 °C (Fig. 2), which is characteristic of hematite (Dunlop and Özdemir 1997). Variable unblocking below 300 °C might be related to progressive dehydration of the samples. No significant remanence loss is observed at 120 °C or 320–350 °C (Fig. 2), which would suggest either the presence of goethite (Özdemir and Dunlop 1996) or magnetic iron sulphide minerals (Dekkers 1989; Roberts 1995), respectively. Above 300 °C, the magnetization gradually unblocks up to 680 °C, which suggests a distribution of hematite grain sizes. These thermal demagnetization results demonstrate that, for the studied sediments at Site 967, the $IRM_{0.9\ T}@AF_{120\ mT}$ parameter is an unambiguous proxy for hematite content.

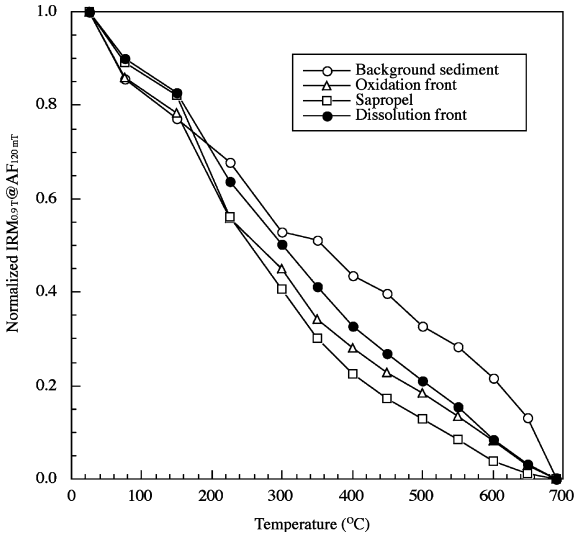

Fig. 2 Thermal demagnetization results of the $IRM_{0.9\ T}@AF_{120\ mT}$ for representative samples from Site 967. The main decay of remanence intensity at ~680 °C indicates that hematite (Dunlop and Özdemir 1997) is the only magnetic mineral that clearly contributes to $IRM_{0.9\ T}@AF_{120\ mT}$. Lack of remanence loss at ~120°, ~320–350° and ~580 °C indicates that goethite (Özdemir and Dunlop 1996), magnetic iron sulphides (Dekkers 1989; Roberts 1995) and magnetite (Dunlop and Özdemir 1997) do not contribute significantly to the $IRM_{0.9\ T}@AF_{120\ mT}$. Representative samples include the range of magnetic behaviours encountered in eastern Mediterranean sediments, including: background sediment (967B-9H-3-47 cm), an oxidation front (967A-3H-4-120 cm), a sapropel (967A-5H-4-46 cm), and a dissolution front (967A-5H-4-53 cm). See Larrasoaña et al. (2003) for a detailed description of the magnetic properties of these different types of sediments

Magnetic, geochemical and oxygen isotope data are shown in Fig. 3 for an interval from ODP Site 967 that has been demonstrated to provide an exceptional record of north African paleoclimate variability (Lourens et al. 2001). A distinctive cyclic pattern is evident in Ti/Al ratios, with minimum values in the sapropels and highest values in the intercalated homogeneous marls. Ti is linked to aeolian transport in the distal marine sediments of Site 967, whereas Al is related to both aeolian (e.g. kaolinite; Foucault and Mélières 2000) and fluvial (e.g. smectite; Lourens et al. 2001) sources. Variations in Ti/Al can therefore be interpreted in terms of the relative contributions of aeolian (Saharan dust) and fluvial (Nile) sources. The Ti/Al record strikingly parallels summer insolation at 65°N and provides the basis for an unambiguous astronomical age calibration (Lourens et al. 2001). The influence of Northern Hemisphere insolation maxima on the eastern Mediterranean hydrography via enhanced monsoon flooding is evident in the sharp negative $\delta^{18}O$ anomalies within most sapropels (Kroon et al. 1998) (Figs. 3 and 4).

Sapropels and underlying sediments (down to 30 cm beneath sapropels) have distinctively low ARM intensities (< 0.05 A/m) that indicate low concentrations of magnetite (Fig. 3). These low magnetite concentrations

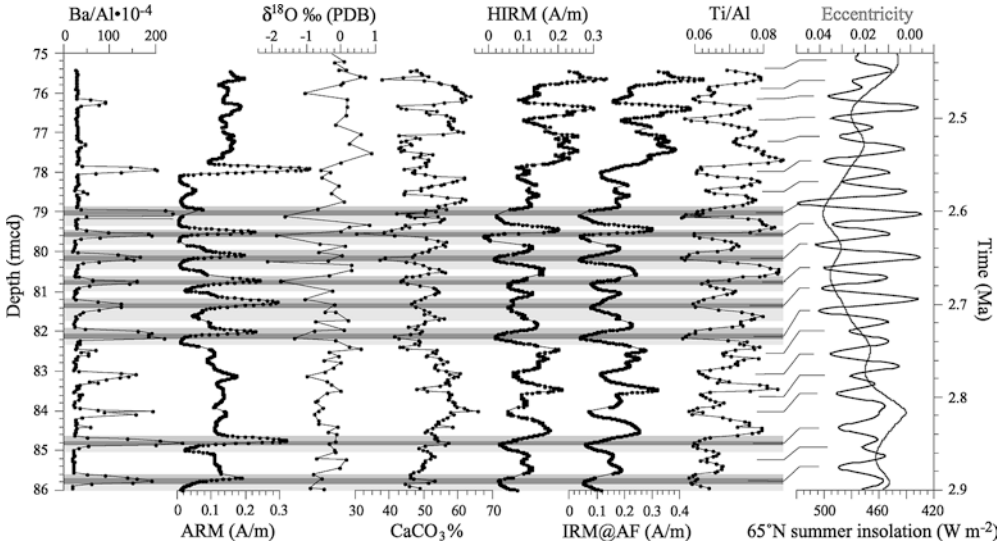

Fig. 3 Geochemical, magnetic and oxygen isotope data from ODP Site 967 between 2.4 and 2.9 Ma, plotted against northern summer insolation and eccentricity (reversed axis) calculated after the astronomical solution of Laskar et al. (1993). *Dark grey shaded bars* indicate the positions of sapropels. *Light grey shading* below and above sapropels indicates the positions of magnetite dissolution and oxidation fronts, respectively (see Larrasoaña et al. 2003 for a comprehensive treatment). The age model is after Lourens et al. (2001). Geochemical (Lourens et al. 2001) and magnetic analyses were carried out on core sections 967A-8H 5 to 7 and 967B-9H 1 to 5, whereas oxygen isotope data were obtained from both holes 967B and 967C (Kroon et al. 1998)

can be explained by pervasive dissolution of magnetite grains within sapropels and underlying sediments that was triggered by downward migration of excess sulphide from the overlying sapropel (Roberts et al. 1999; Kruiver and Passier 2001; Passier et al. 2001; Larrasoaña et al. 2003). ARM intensities higher than background levels ($\backsim$0.1 A/m) are found up to 15 cm above sapropels (Fig. 3). This is consistent with the post-depositional formation of (possibly biogenic) fine-grained magnetite at oxidation fronts developed above the sapropels (Passier et al. 2001; Kruiver and Passier 2001; Larrasoaña et al. 2003). Magnetic proxies for hematite content at Site 967 (HIRM and $IRM_{0.9\ T}@AF_{120\ mT}$) closely agree with the Ti/Al curve regardless of non-steady-state diagenetic processes around sapropels and changes in $CaCO_3$ concentration (Fig. 3), which suggests that it has not been significantly affected by diagenesis. Hematite can form aggregates and/or intergrowths with silicates and other material incorporated into the dust and could therefore remain protected against reductive dissolution within sapropels and dissolution fronts (Kruiver and Passier 2001). Because of its expression in terms of an absolute hematite content, the $IRM_{0.9\ T}@AF_{120\ mT}$ parameter offers improved quantitative insights into the history of dust deposition compared to the Ti/Al ratios that reflect only relative shifts between aeolian and fluvial sediment supply.

4 Discussion

The dominance of hematite in the high-coercivity fraction at Site 967 (Fig. 2) indicates that the dust source lies in the Saharan region where warm and dry conditions favour formation of hematite (Maher 1986), rather than the Sahel where relatively wetter conditions favour formation of goethite (Balsam et al. 1995). The hematite in the dust is likely to occur as a result of the sum of past Saharan climate and weathering regimes, which frequently changed between relatively humid (green Sahara) and arid conditions. Hard, goethite-rich iron crusts formed during previous wetter phases (Nahon 1980), and hematite would have formed as a result of secondary alteration of these goethite-rich iron crusts during arid climate phases. The source region within the Sahara can be further constrained to the northern sector ($>$21°N), since dust produced in the southern sector is mainly removed toward and over the North Atlantic by the African easterly jet (Prospero 1996; Goudie and Middleton 2001). Additional evidence for a northern Saharan provenance comes from the occurrence of palygorskite (Foucault and Mélières 2000) and ^{87}Sr-enriched material (Krom et al. 1999; Weldeab et al. 2002) in central and eastern Mediterranean sediments, and from the known importance of northward transport of Saharan dust by low altitude ($<$2000 m) winds (Dayan et al. 1991). We therefore argue that the main source areas of dust delivered to the eastern Mediterranean Sea are the lowlands of eastern Algeria, Libya and western Egypt, between $\backsim$21 and 30°N. These regions contain fossil river and lake deposits and host a system of wadis that are sourced from the Ahaggar, Tibesti and Ennedi ranges (Gaven et al. 1981; Pachur and Hoelzmann 2000; Rohling et al. 2001; Wadi Kufra radar image 2002) (Fig. 1). The easily weathered and deflated silt-rich alluvium from these areas fuels the bulk of modern dust

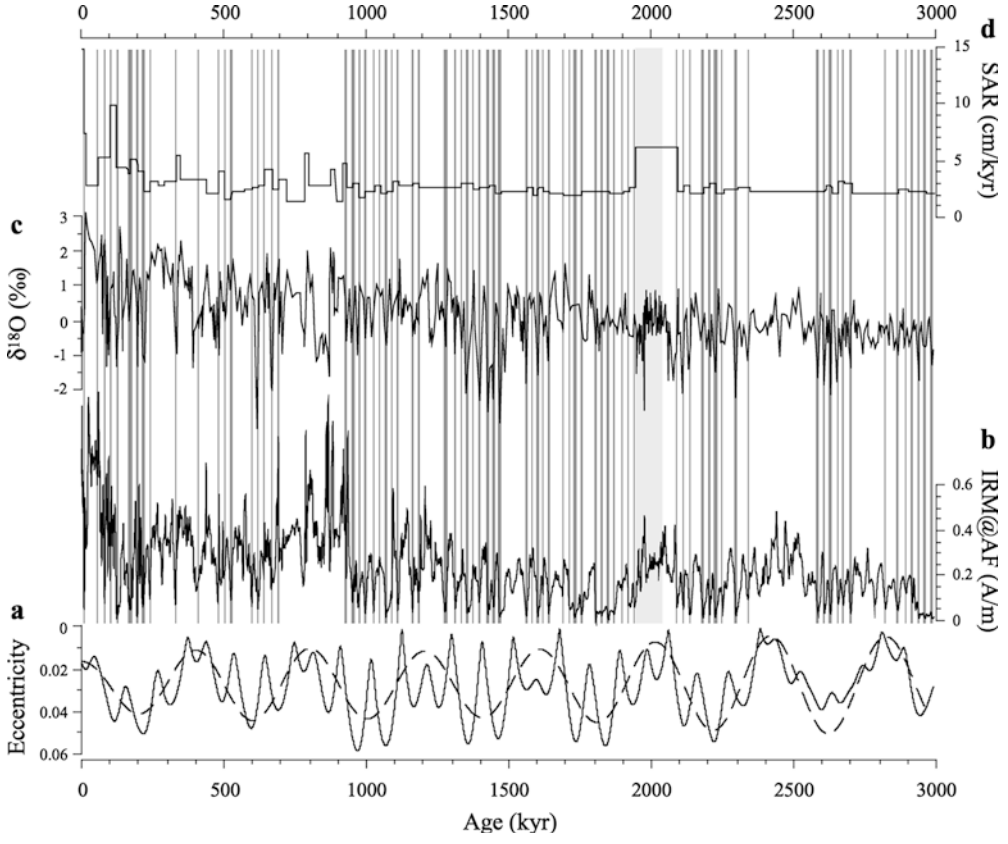

Fig. 4 **a** Variations of orbital eccentricity for the last 3 million years (the *dashed line* is the 400-kyr component of eccentricity) from the astronomical solution of Laskar et al. (1993). **b** Down-core variations of $IRM_{0.9\ T}@AF_{120\ mT}$ for ODP Site 967, which indicate variations in hematite concentration as a proxy for Saharan dust supply. **c** Oxygen isotope record for Site 967 (Kroon et al. 1998). **d** Down-core variations of sediment accumulation rates (SAR). The *dark grey shaded bars* indicate the positions of sapropels and the *light grey shaded bar* at ~2 Ma marks the position of a slumped interval

production (Goudie and Middleton 2001). Northern Saharan dust is delivered into the easternmost Mediterranean Sea mainly in late winter and spring, in connection with the activity of Mediterranean depressions (Dayan et al. 1991; Goudie and Middleton 2001). The dust is transported northward at the eastern (warm) side of these depressions, while cold, high-latitude air invades the Mediterranean basin at the western side of the fronts (Fig. 5). The calcrete-rich (hematite-poor) areas of the northwestern Sahara (Sarnthein et al. 1981), which could complicate interpretation of our record, are not considered to significantly contribute to dust supply in the eastern Mediterranean because dust outbreaks emanating from this region are mainly transported over the North Atlantic (Prospero 1996) or into the western Mediterranean (Dayan et al. 1991; Goudie and Middleton 2001).

Stratigraphic variations of the $IRM_{0.9\ T}@AF_{120\ mT}$ parameter for Site 967 are shown in Fig. 4 together with $\delta^{18}O$ data (Kroon et al. 1998). With few exceptions, sapropels have distinctly low hematite contents and $\delta^{18}O$ values, which contrast with higher values for both parameters in the intercalated marls. The correspondence between hematite contents and $\delta^{18}O$ values is suggestive of a pervasive control on both parameters, throughout the last 3 million years, by northward penetration of the African summer monsoon beyond the central Saharan watershed (~21°N) at times of sapropel formation (precession minima), as proposed previously for Eemian sapropel S5 (Rohling et al. 2002). The associated monsoon flooding into the eastern Mediterranean from both the Nile and the wider north African margin would have resulted in reduced surface-water salinities, which, in turn, inhibited bottom-water ventilation and so created conditions conducive to sapropel formation (Rohling 1994; Myers et al. 1998).

Beside these variations on precession time scales, we also observe long-term cycles in our dust record (Figs. 4, 6, 7, 8; Table 1). Most notably, we find broad intervals of high and low hematite fluxes that coincide with 400-kyr eccentricity minima and maxima, respectively (Fig. 4). The 100-kyr eccentricity cycles are also present in our dust record, albeit with considerably weaker expressions (Figs. 4, 6, 7, 8). The presence of both eccentricity periods suggests that the northward penetration of the African summer monsoon front beyond 21°N during northern summer insolation maxima is subject to long-term modulation by orbital eccentricity, as might be expected from its influence on the impact of the precession cycle on insolation. Amplification of the

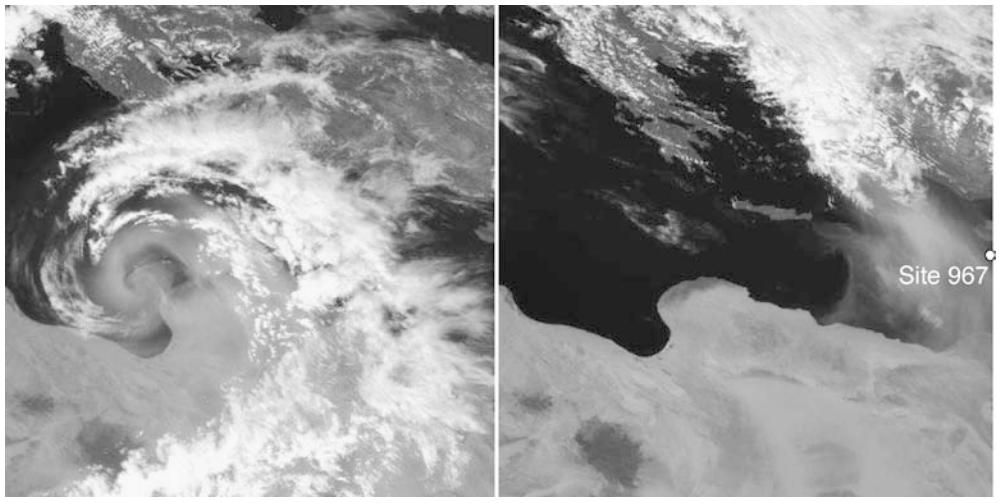

Fig. 5 Satellite image (from Meteosat-7) of an Eastern Mediterranean dust outbreak on 17 (*left*) and 18 (*right*) April, 2001 (both taken at 12:00 UTC). A large dust cloud is evident in association with a synoptic system that is still recognizable on 17 April. On 18 April, the system is no longer visible but the cloud had travelled some distance toward the eastern Mediterranean. *ODP Site 967* is shown at the edge of the *right-hand image*, near the leading edge of the dust cloud. From http://www.eumetsat.de/en/area5/special/duststorm_042001.html, December 2002

impact of precession during eccentricity maxima would increase the potential for the African summer monsoon front to penetrate to the north of the central Saharan watershed at ~21°N and would consequently lead to the enhanced soil moisture and vegetation cover that inhibit dust production. Conversely, dampening of the impact of precession during eccentricity minima would reduce the potential of the African summer monsoon front to penetrate beyond the watershed and consequently favour the persistently dry, non-vegetated, desert conditions (Claussen et al. 1998; Brovkin et al. 1998) that are conducive to elevated dust production. This interpretation of the influences of eccentricity is consistent with the observation that the long eccentricity cycles in the dust record show broad agreement with long-term variations in eastern Mediterranean bottom-water ventilation, as deduced from diagenetically-controlled variations in geochemical and magnetic properties in the sediments at Site 967 (Larrasoaña et al. 2003). With enhanced monsoon penetration, greater monsoon flooding would affect the eastern Mediterranean by reducing surface salinities, thereby inhibiting deep-water ventilation. This relationship is also illustrated by the coincidence of large-scale clusters of sapropels (within 400-kyr eccentricity maxima) with the lightest $\delta^{18}O$ anomalies and lowest hematite contents (Figs. 3 and 4). We emphasise that the recurrence of elevated productivity, indicated by high Ba/Al ratios (Thomson et al. 1995), does not seem to have been affected by variations on eccentricity time scales (Fig. 3). This strongly suggests a primary control of long-term variations in bottom-water ventilation (Larrasoaña et al. 2003) on the formation and/or preservation of sapropels.

It is worth observing that the relationship between high dust fluxes and eccentricity minima for dust sourced from the northern Sahara contrasts with equatorial Atlantic records of dust sourced from the southern Sahara–Sahel, where eccentricity minima coincide with low dust fluxes (Tiedemann et al. 1994). Conversely, the responses of both records appear to be similar on precession time scales, where dust minima generally coincide with precession minima. The observed long-term (10^5-year) contrast and shorter-term (10^4-year) similarity between the near-equatorial and subtropical dust records present a challenge to the modelling of paleoclimate evolution on orbital time scales. Such models will need to include changes in ice volume and its global distribution, soil conditions, vegetation cover, feedback mechanisms, and atmospheric circulation with its highly seasonal variability.

Visual inspection, spectral analyses and band-pass filtering of the dust record from Site 967 indicate that the precession- and eccentricity-related variations in northern Saharan dust supply are well expressed in the record, despite an overall increase in the dust supply at the mid-Pleistocene transition at ~0.95 Ma (Figs. 4, 6, 7, 8; Table 1). Apparently, cyclic penetration of the African summer monsoon into the northern Sahara continued

Table 1 Percentage of variance of the Site 967 dust record explained by orbital components

Age interval (Ma)	Precession	Obliquity	Short eccentricity	Long eccentricity	Total orbital[a]	Sub-Milankovitch periods	
Filter band	18–25 kyr	39–43 kyr	90–130 kyr	394–414 kyr		9–15 kyr	4–8 kyr
0–1	7.5	2.1	4.6	5.7	19.3	10.6	4.5
1–2	6.4	22.1	12.5	6.9	49.6	4.3	1.8
2–3	9.9	14.8	3.9	19.5	47.9	2.7	0.7

[a]The total is the variance explained by a signal composed only of the four listed Milankovitch components. The total takes into account the phase of the signal and therefore may not equal the sum of the individual components

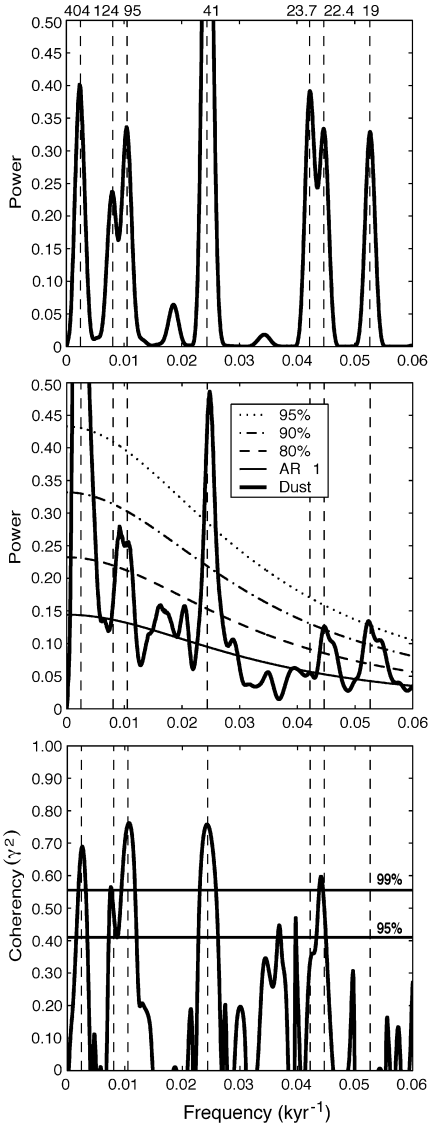

Fig. 6 Estimated power spectrum of the astronomical solution of Laskar et al. (1993) (*top*), the ODP Site 967 $IRM_{0.9\ T}@AF_{120\ mT}$ record for 0–3 Ma (*middle*), and their estimated coherency (*bottom*). Each spectrum represents an average over seven Hanning-tapered segments with 50% overlap. The power spectra are normalised so that $IRM_{0.9\ T}@AF_{120\ mT}$ 404-kyr = 1 and La93(1, 1) 41-kyr = 1. The significance of spectral peaks in the dust record is tested against the null hypothesis of a first-order autoregressive (AR-1) process (Mann and Lees 1996). 80%, 90% and 95% confidence levels were calculated from the best-fitting red-noise background due to an AR-1 process with persistence time of 2.8 kyr. The estimated coherence was bias-corrected (Schulz and Stategger 1997) and confidence levels were calculated under the null hypothesis of two uncorrelated random processes. Orbital forcing of the dust record is clearly demonstrated, with statistically significant coherency between the orbital solutions and dust fluctuations at Site 967

throughout the progressive build-up of Northern Hemisphere ice sheets between 3 Ma and the present. However, we note that both deep dust minima and sapropel occurrences became less abundant since 0.95 Ma (Fig. 4), which suggests a stronger tendency for the monsoon front to remain south of the watershed after 0.95 Ma. Sufficient northward penetration of the monsoon then became restricted to high-amplitude insolation maxima. Since the mid-Pleistocene transition, when the amplitude of Northern Hemisphere ice sheet variations became larger (Tiedemann et al. 1994), we also observe a strong increase in the variability of the dust record at sub-Milankovitch time scales, although it is not clearly organized in distinct frequency bands (Figs. 7, 8; Table 1). This suggests that a causal relationship may exist between the magnitude of Northern Hemisphere ice sheets and the expression of millennial scale climate variability in our subtropical dust record, possibly through changes in the Northern Hemisphere's meridional temperature gradient.

Finally, we observe strong spectral power in the dust record at the 41-kyr obliquity period prior to ~0.95 Ma (Figs. 7, 8) and a developing recurrence of this period since ~0.3 Ma, consistent with the 1.2-Myr modulation of obliquity in the astronomical records (Laskar et al. 1993) (Fig. 8). The phase relationship between the 41-kyr component of the dust record and the orbital obliquity variations consistently links low dust fluxes with high obliquity (Fig. 8). The strong high latitude influence of obliquity would have affected the Southern Hemisphere's meridional temperature gradient in austral winter (high obliquity = enhanced temperature gradient), which would influence the boreal summer monsoon intensity/penetration (Pedelaborde 1963; Rossignol-Strick 1985; Rohling et al. 2002). Furthermore, there may be some degree of low latitude control by obliquity on the supply of Saharan dust into the eastern Mediterranean, through-changes in the latitude of the tropics (the highest latitudes at which the sun reaches its zenith directly overhead) between latitudes of 22.0° at obliquity minima and 24.5° at maxima. The associated change in the amplitude of the annual swing of the thermal equator may not be apparent in most (sub)tropical settings. However, the particular setting investigated here involves a critical watershed at around 21°N that makes it susceptible to a threshold-type response to what would otherwise seem a minor latitudinal change in the African summer monsoon penetration.

5 Conclusions

We have produced the first continuous high-resolution record of Saharan dust deposition in the eastern Mediterranean for the last 3 million years, based on hematite contents derived from magnetic properties of sediments from ODP Site 967. We relate variations in the dust supply to climatic changes in source areas located north of the central Saharan watershed. Distinct dust minima coincide with Northern Hemisphere insolation maxima, which is consistent with enhanced northward penetration of the African summer monsoon front across the central Saharan watershed at those times. On precession time scales, variations in our subtropical dust record are similarly phased to those in equatorial Atlantic records

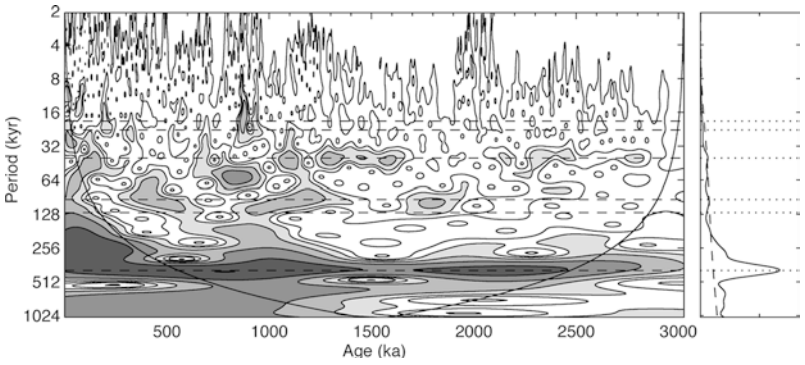

Fig. 7 Wavelet power spectrum (*left*) and the global wavelet spectrum (*right*) for the ODP Site 967 dust record. Note that, compared to Fig. 6, longer periods are over-emphasised in a wavelet power spectrum. Contours filled with *shaded tones* indicate areas with power above the 95% confidence level. *Curved lines* on either side of the wavelet power spectrum indicate the "cone of confidence" where edge effects become important. *The dashed lines in the wavelet power spectrum* represent the main orbital periods for precession, obliquity and eccentricity, respectively. The *dashed line in the global spectrum* is the 95% confidence limit, while the *dotted lines* indicate the main orbital periods

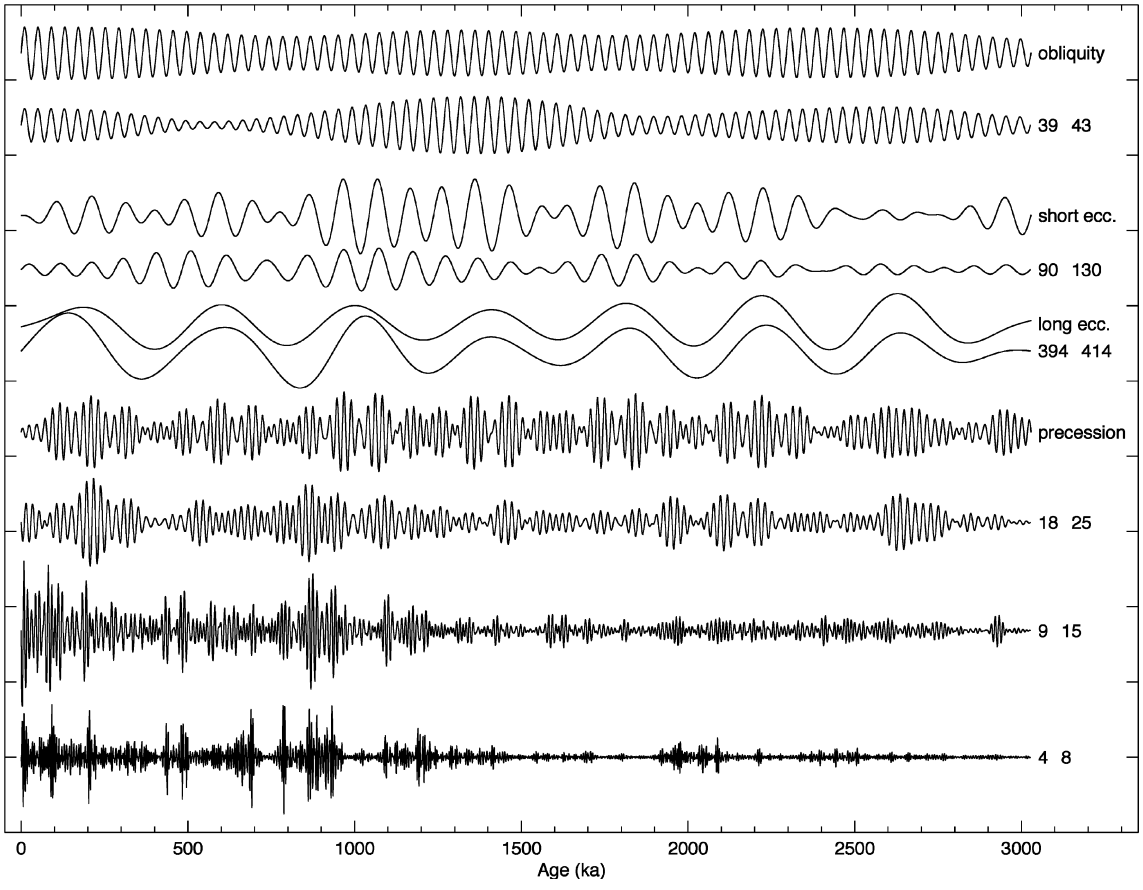

Fig. 8 Comparison of the band-pass-filtered $IRM_{0.9\ T}@AF_{120\ mT}$ dust record for ODP Site 967 (the period bands are stated in kyr) with the solution for orbital parameters from Laskar et al. (1993). The La93(1, 1) solution was band-pass filtered using the same band as the dust record, and normalized by the respective standard deviation. The scaling factor for the band-pass-filtered dust signal is the same for all period bands so as to conserve the relative amplitude ratios between the band-pass components of the signal. The band-pass filtered signals were multiplied by –1 to illustrate the anti-correlation between dust production and insolation. The results show the clear 1.2-Myr modulation of the 41-kyr obliquity cycle

of dust sourced from the southern Sahara-Sahel (Tiedemann et al. 1994). However, on eccentricity time scales, the responses are distinctly anti-phased between these two regions. This contrast offers a significant new constraint to simulations of paleoclimate on orbital timescales.

Despite the fact that our record is from a low-latitude site, we observe distinct variability on obliquity time scales. Moreover, there is a persistent phase relationship between the 41-kyr component of the dust record and the orbital obliquity variations that link low dust fluxes with high obliquity. We suggest that the expression of obliquity results from a high-latitude mechanism driven from the Southern Hemisphere and/or a low-latitude mechanism associated with a sensitive threshold response of dust production in the northern Sahara to relatively minor shifts in the latitude of the tropics.

Sub-Milankovitch variability is poorly expressed in the dust record prior to the mid-Pleistocene transition ($\backsim$0.95 Ma). At the mid-Pleistocene transition, when the amplitude of Northern Hemisphere ice volume variations increased, there was a marked increase in this expression. This suggests that millennial-scale climate variability, including monsoon dynamics, is linked to the size of Northern Hemisphere ice sheets.

Acknowledgements We thank the staff from the ODP Core Repository in Bremen for technical assistance and hospitality during sampling. We also thank Catherine Kissel, Michael Sarnthein and two anonymous reviewers for their constructive comments that helped to improve the paper and Jean-Claude Duplessy for editorial handling. This work was financially supported by European Community TMR Network contract MAG-NET (ERBFMRXCT98-0247) and the UK NERC, and contributes to NERC project NER/B/S/2002/00268. Samples were provided by the ODP, which is sponsored by the US National Science Foundation and participating countries (including the UK) under management of Joint Oceanographic Institutions, Inc.

References

Balsam WL, Otto-Bliesner BL, Deaton BC (1995) Modern and last glacial maximum eolian sedimentation patterns in the Atlantic Ocean interpreted from sediment iron oxide content. Paleoceanography 10: 493–507

Brovkin V, Claussen M, Petoukhov V, Ganopolski A (1998) On the stability of the atmosphere-vegetation system in the Sahara/Sahel region. J Geophys Res 103: 31,613–31,624

Claussen M, Brovkin V, Ganopolski A, Kubatski C, Petoukhov V (1998) Modelling global terrestrial vegetation-climate interaction. Philos Trans R Soc London 353: 53–63

Dayan U, Heffter J, Miller J, Gutman G (1991) Dust intrusions into the Mediterranean basin. J Appl Meteorol 30: 1185–1199

Dekkers MJ (1989) Magnetic properties of natural pyrrhotite. II. High- and low-temperature behaviour of *Jrs* and TRM as function of grain size. Phys Earth Planet Inter 57: 266–283

Dinarès-Turell J, Hoogakker BAA, Roberts AP, Rohling EJ, Sagnotti L (2003) Quaternary climatic control of biogenic magnetite production and eolian dust input in cores from the Mediterranean Sea. Palaeogeogr Palaeoclimatol Palaeoecol 190: 195–209

Dunlop DJ, Özdemir Ö (1997) Rock magnetism: fundamentals and frontiers. Cambridge University Press, New York, pp 573

Emeis K-C, Sakamoto T, Wehausen R, Brumsack H-J (2000) The sapropel record of the eastern Mediterranean Sea – results of Ocean Drilling Program Leg 160. Palaeogeogr Palaeoclimatol Palaeoecol 158: 371–395

Emeis K-C, Schulz H, Struck U, Rossignol-Strick M, Erlenkeuser H, Howell MW, Kroon D, Mackensen H, Ishizuka S, Oba T, Sakamoto T, Koizumi I (2003) Eastern Mediterranean surface water temperatures and δ^{18}O composition during deposition of sapropels in the late Quaternary. Paleoceanography 18: doi: 10.1029/2000PA000617

Fontugne M, Arnold M, Labeyrie L, Calvert SE, Paterne M, Duplessy JC (1994) Palaeoenvironment, sapropel chronology and Nile River discharge during the last 20,000 years as indicated by deep sea sediment records in the eastern Mediterranean. Radiocarbon 34: 75–88

Foucault A, Mélières F (2000) Palaeoclimatic cyclicity in central Mediterranean Pliocene sediments: the mineralogical signal. Palaeogeogr Palaeoclimatol Palaeoecol 158: 311–323

Gasse F (2000) Hydrological changes in the African tropics since the Last Glacial Maximum. Quat Sci Rev 19: 189–211

Gaven C, Hillaire-Marcel C, Petit-Maire N (1981) A Pleistocene lacustrine episode in southeastern Libya. Nature 290: 131–133

Goudie AS, Middleton NJ (2001) Saharan dust storms: nature and consequences. Earth Sci Rev 56: 179–204

King JW, Channell JET (1991) Sedimentary magnetism, environmental magnetism, and magnetostratigraphy. Rev Geophys Suppl 29: 258–370

Krom MD, Cliff RA, Eijsink LM, Herut B, Chester R (1999) The characterisation of Saharan dust and Nile particulate matter in surface sediments from the Levantine basin using Sr isotopes. Mar Geol 155: 319–330

Kroon D, Alexander I, Little M, Lourens LJ, Matthewson A, Robertson AHF, Sakamoto T (1998) Oxygen isotope and sapropel stratigraphy in the Eastern Mediterranean during the last 3.2 million years. In: Robertson AHF, Emeis K-C, Richter C, Camerlenghi A (eds) Proc ODP Sci Res 160, pp 181–190, Ocean Drilling Program, College Station, Texas

Kruiver PP, Passier HF (2001) Coercivity analysis of magnetic phases in sapropel S1 related to variations in redox conditions, including an investigation of the S-ratio. Geochem Geophys Geosys 2: Paper #2001GC00018

Larrasoaña JC, Roberts AP, Stoner JS, Richter C, Wehausen R (2003) A new proxy for bottom-water ventilation in the eastern Mediterranean based on diagenetically controlled magnetic properties of sapropel-bearing sediments. Palaeogeogr Palaeoclimatol Palaeoecol 190: 221–242

Laskar J, Joutel F, Boudin F (1993) Orbital, precessional and insolation quantities for the Earth from –20 Myr to + 10 Myr. Astron Astrophys 270: 522–533

Liu QS, Banerjee SK, Jackson MJ, Zhu RX, Pan YX (2002) A new method in mineral magnetism for the separation of weak antiferromagnetic signal from a strong ferrimagnetic background. Geophys Res Lett 29: 1565–1568

Lourens LJ, Wehausen R, Brumsack H-J (2001) Geological constraints on tidal dissipation and dynamical ellipticity of the earth over the past three million years. Nature 409: 1029–1033

Maher BA (1986) Characterisation of soils by mineral magnetic measurements. Phys Earth Planet Inter 42: 76–92

Mann ME, Lees JM (1996) Robust estimation of background noise and signal detection in climatic time series. Clim Change 33: 409–445

Middleton NJ (1985) Effect of drought on dust production in the Sahel. Nature 316: 431–434

Myers PG, Haines K, Rohling EJ (1998) Modelling the paleo-circulation of the Mediterranean: the last glacial maximum and the Holocene with emphasis on the formation of sapropel S1. Paleoceanography 13: 586–606

Nahon D (1980) Soil accumulations and climatic variations in western Sahara. Palaeoecology of Africa and of the Surrounding Islands and Antarctica (Balkema, Cape Town, South Africa) 12: 63–68

Özdemir Ö, Dunlop DJ (1996) Thermoremanence and Néel temperature of goethite. Geophys Res Lett 23: 921–924

Pachur HJ, Hoelzmann P (2000) Late Quaternary paleoecology and paleoclimates of the eastern Sahara. J Afr Earth Sci 30: 929–939

Passier HF, de Lange GJ, Dekkers MJ (2001) Magnetic properties and geochemistry of the active oxidation front at the youngest sapropel in the eastern Mediterranean Sea. Geophys J Int 145: 604–614

Pedelaborde P (1963) The monsoon. Methuen, London, pp 196

Prospero JM (1996) Saharan dust transport over the North Atlantic Ocean and Mediterranean: an overview. In: Guerzoni S, Chester R (eds) The impact of desert dust across the Mediterranean. Kluwer Academic Publishing, Dordrecht, pp 133–151

Roberts AP (1995) Magnetic characteristics of sedimentary greigite (Fe_3S_4). Earth Planet Sci Lett 134: 227–236

Roberts AP, Stoner JS, Richter C (1999) Diagenetic magnetic enhancement of sapropels from the eastern Mediterranean Sea. Mar Geol 153: 103–116

Rohling EJ (1994) Review and new aspects concerning the formation of eastern Mediterranean sapropels. Mar Geol 122: 1–28

Rohling EJ, Cane TR, Cooke S, Sprovieri M, Bouloubassi I, Emeis K-C, Schiebel R, Kroon D, Jorissen FJ, Lorre A, Kemp AES (2002) African monsoon variability during the previous interglacial maximum. Earth Planet Sci Lett 202: 61–75

Rossignol-Strick M (1983) African monsoons, an immediate climate response to orbital insolation. Nature 304: 46–49

Rossignol-Strick M (1985) Mediterranean Quaternary sapropels, an immediate response of the African monsoon to variation of insolation. Palaeogeogr Palaeoclimatol Palaeoecol 49: 237–263

Rossignol-Strick M, Nesteroff W, Olive P, Vergnaud-Grazzini C (1982) After the deluge; Mediterranean stagnation and sapropel formation. Nature 295: 105–110

Sakamoto T, Janecek T, Emeis K-C (1998) Continuous sedimentary sequences from the eastern Mediterranean Sea: composite depth sections. In: Robertson AHF, Emeis K-C, Richter C, Camerlenghi A (eds) Proc ODP Sci Res 160, pp 37–59, Ocean Drilling Program, College Station, Texas

Sarnthein M, Tetzlaff G, Koopmann B, Wolter K, Pflaumann U (1981) Glacial and interglacial wind regimes over the eastern subtropical Atlantic and NW Africa. Nature 293: 153–157

Schulz M, Stattegger K (1997) SPECTRUM: Spectral analysis of unevenly spaced paleoclimatic time series. Comp Geosci 23: 929–945

Shipboard Scientific Party (1996) Site 967. In: Robertson AHF, Emeis K-C, Richter C (eds) Proc ODP Init Repts 160, pp 215–287, Ocean Drilling Program, College Station, Texas

Staerker TS (1998) Quantitative calcareous nannofossil biostratigraphy of Pliocene and Pleistocene sediments from the Eratosthenes Seamount region in the eastern Mediterranean. In: Robertson AHF, Emeis K-C, Richter C, Camerlenghi A (eds) Proc ODP Sci Res 160, pp 83–98, Ocean Drilling Program, College Station, Texas

Thomson J, Higgs NC, Wilson TRS, Croudace IW, de Lange GJ, van Santvoort PJM (1995) Redistribution and geochemical behavior of redox-sensitive elements around S1, the most recent eastern Mediterranean sapropel. Geochim Cosmochim Acta 59: 3487–3501

Tiedemann R, Sarnthein M, Shackleton NJ (1994) Astronomic time scale for the Pliocene Atlantic $\delta^{18}O$ and dust flux records of Ocean Drilling Program site 659. Paleoceanography 9: 619–638

Torrence C, Compo GP (1998) A practical guide to wavelet analysis. Bull Am Meteorol Soc 79: 61–78

Wadi Kufra radar image. http://southport.jpl.nasa.gov/imagemaps/html/srl-wadik.html. Image P-45719, December 2002

Weeks R, Laj C, Endignoux L, Fuller M, Roberts A, Manganne R, Blanchard E, Goree W (1993) Improvements in long-core measurement techniques: applications in palaeomagnetism and palaeoceanography. Geophys J Int 114: 651–662

Wehausen R, Brumsack H-J (2000) Chemical cycles in Pliocene sapropel-bearing and sapropel-barren eastern Mediterranean sediments. Palaeogeogr Palaeoclimatol Palaeoecol 158: 325–352

Weldeab S, Emeis K-C, Hemleben C, Siebel W (2002) Provenance of lithogenic surface sediments and pathways of riverine suspended matter in the eastern Mediterranean Sea: evidence from $^{143}Nd/^{144}Nd$ and $^{87}Sr/^{86}Sr$ ratios. Chem Geol 186: 139–149